The 11th International Conference on Hydrogen Production (ICH2P-2020)

5- 9 July 2020, Istanbul, Turkey
TOPIC - Hydrogen storage and materials

SYNTHESIS AND CHARACTERISTICS OF MAGNETITE CONTAINING-CMK-3 AND ITS APPLICATION IN HYDROGEN STORAGE

Juliana Juarez, Lisandro Venosta, Marcos Gómez Costa and Oscar A. Anunziata
National Technological University, Faculty of Córdoba – NANOTEC - Córdoba-ARGENTINA

Abstract

In this work, we report the synthesis and characterization of iron oxide nanoparticles (Magnetite) supported on CMK-3. The materials were characterized by XRD, SEM, TEM, XPS and magnetization studies. A large amount of the iron incorporated as iron oxide nanoparticles was in the magnetite phase. The incorporation of magnetite on the CMK-3 carbon surface significantly improved the hydrogen storage capacity (4.45 wt. % at 77 K and 10 bar) compared to the CMK-3 structure (2.20 wt% at 77 K and 10 bar). Magnetite nanoparticles play a key role in H2 adsorption.

Keywords: Magnetite, CMK-3, Hydrogen Storage

1. INTRODUCTION

The incorporation of metal nanoparticles or metal oxides promotes the presence of viable active sites for H2 adsorption [1]. Nanoparticles dispersed in the pores of nanostructured carbons are the key to improving hydrogen storage capacity. Although metals such as platinum or palladium have been shown to improve the behavior of this mechanism, other studies present better results using cheaper metals [2]. It is clear that the hydrogen adsorption capacity of carbon materials can be improved with the introduction of suitable nanoparticles. Although the proportionality of hydrogen storage was found to be more dependent on the specific surface area, the micropore diameter plays a key role in the final storage [3]. In previous reports, employing Pt, Ni, Zn, TiO2, and V2O5 nanoparticles among others, incorporated in nanostructured carbon CMK-3 we have shown higher hydrogen uptake at lower and higher pressures than CMK-3 [4 - 7]. In this framework, the present work aims to study the hydrogen

storage capacity of material to Magnetite ported on CMK-3.

2. EXPERIMENTAL

Magnetite nanoparticle modified material (Fe- CMK-3) was prepared by wet impregnation using FeCl3-6H2O as the iron source. This source was dissolved in deionized water and the CMK-3 support [4], was incorporated into this solution. The mixture was placed in a rotary evaporator to remove excess water at 60 °C and 60 rpm. at 60 °C and 60 rpm. The sample was then dried at 100 °C overnight. Finally, the modified mesoporous carbon was desorbed in an inert atmosphere (inert gas).
The modified mesoporous carbon was desorbed in an inert atmosphere (N2, 20 mL/min) at 550 °C for 4 h. The percentage of incorporated iron was ~2 wt.%, according to ICP measurements.
Elemental analysis was performed by inductively coupled plasma-atomic emission spectroscopy (ICP) in a VISTA-MPX spectrometer. The X-ray diffractogram was obtained with a Panalytical Philips X'pert XDS diffractometer. BET adsorption-desorption isotherms and pore size distribution were measured in a high-speed gas sorption analyzer (Nova 4000) after outgassing the samples at 200 °C for 4 h with reproducibility of ± 0.5%. The pore size distribution (PSD) was estimated using the nonlocal density functional theory (NLDFT) algorithm from adsorption isotherms. TEM micrographs were taken in a TEM Philips EM 301 instrument. Magnetic properties measurements of the samples were performed with a Lakeshore 7300 vibrating sample magnetometer (VSM). Scanning electron microscopy images were obtained with a FE-SEM, Sigma Zeiss equipment. XPS measurements were performed in a K-Alpha™ + X-ray photoelectron spectrometer (XPS). The spectrum was calibrated to the binding energy of the C–C carbon signal. Hydrogen storage isotherms at 77 K at low and high pressure (up to 10 bar) was measured using ASAP 2050 equipment properlycalibrated.

3. RESULTS Y DISCUSSION

X-ray diffraction

The low-angle X-ray diffractograms of CMK-3 and Fe-CMK-3 show a comparable structural order with P6mm, while for Fe-CMK-3 it shifts to higher angles due to the oxide incorporation in the CMK-3 channels, with the magnetite nanoparticles generating a slight alteration in the uniformity of the channels.
High-angle X-ray diffractograms of the iron-modified material before (Fe-CMK-3) and after (Fe-CMK-3-H) hydrogen adsorption measurements are shown in Figure 1. Typical (002) and (100) reflections of graphitic carbons [8], are observed along with reflections characteristic of magnetite (Fe3O4) spinel iron oxide: (220), (311), (400), (422), (511) and (440), (PDF2 database: 00-019-0629). Magnetite nanoparticles with a crystal size of approximately 18 nm for both samples, based on the estimation of

the Scherrer equation, without disturbing the Carbons Structure, together with the null influence of H2 on Magnetite.

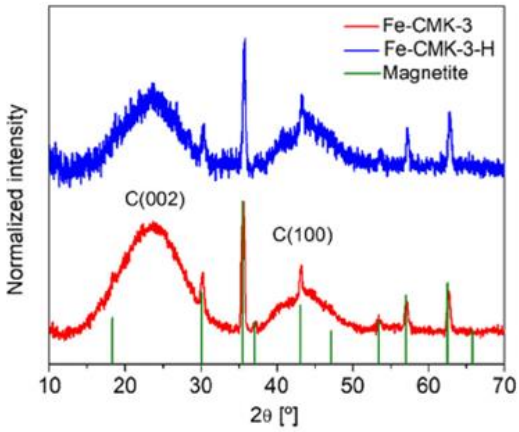

Figure 1: XRD at high angle of Fe-CMK-3 and Fe-CMK-3-H

Textural properties

CMK-3 and Fe-CMK-3 nitrogen adsorption/desorption isotherms (before and after hydrogen adsorption test) at 77 K shows a type IV H2 behavior with physisorption hysteresis, according to the typical IUPAC catalog of ordered nanoporous materials.

The iron samples show a lower specific surface area and pore size compared with CMK-3 (CMK-3 1323 m2/g, 1.01mL/g and 4.2nm pore diameter, whereas for Fe-CMK-3, 1237m2/g; 0.980mL/g and 3.6nm Respectively, which point to that magnetite nanoparticles are within the mesoporous channels of the CMK-3 framework.

SEM and TEM studies

SEM images of Fe-CMK-3 indicate (Supplementary Material Slide 4), the average particle size D ~ 40 nm (polycrystalline), obtained by statistical analysis of several images, comparable with the particle size estimated by the Scherrer equation.

The TEM image (Supplementary Material Slide 5), shows that the average particle size was D ~ 4 nm (Figure 2), in contrast to the larger particle size detected by SEM (D ~ 40 nm) located on the outer surface.

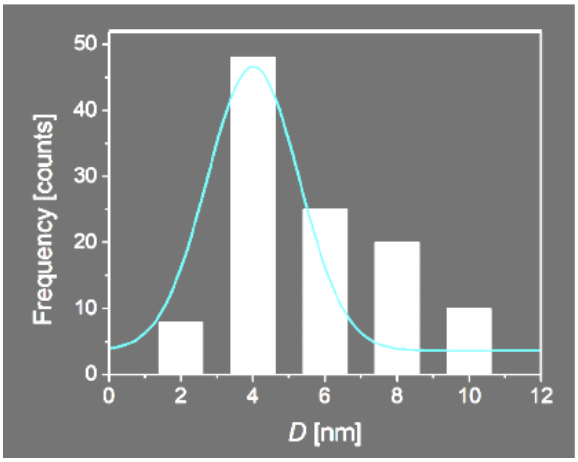

Figure 2: Particle size distribution analysis

XPS

The XPS results of the Fe-CMK-3 sample are given in Table 1. In the case of CMK-3, the EB of C1s at approximately 284 and 286 eV are attributed to C-C sp3 a and C=C sp2, characteristic of graphite and disordered carbon species, [9].

The full XPS spectrum of Fe-CMK-3 (Supplementary Material Slide 6) and Table 1 show signals around 724.8 eV and 711.8 eV corresponding to the doublet of the 2p1/2 and 2p3/2 signals of magnetite (Fe3O4). The characteristic C-O bands and the one corresponding to the O bound to the metal cations (magnetite) are also observed. The low amount of iron oxide on the surface suggests that the iron species are found mainly in the internal channels of the mesoporous carbon. The Fe 2p of approximately 1.4 wt. % (see Table 1), indicates that iron is well distributed both on the surface and inside the CMK-3 channels. Based on the ICP results for the iron content (1.98 wt.%), it is possible to infer that there is a greater amount of magnetite nanoparticles smaller inside the channels than outside, where larger nanoparticles are found. The Fe/C atomic ratio is 0.003 (2% error), which would indicate that the magnetite is highly dispersed within the carbonaceous material.

Table 1 Binding energy (BE), at.% and wt% of C, O, and Fe in Fe-CMK-3

	BE (eV)	at.%	wt%
C1s	284.78	96.06	93.88
	286.28		
	287.48		
	289.88		
O1s	531.18	3.63	4.73
	533.48		
	536.33		
Fe 2p	711.93	0.31	1.39
	725.03		

Magnetic properties

The curve obtained corresponds to a ferromagnetic signal consistent with the presence of magnetite (Supplementary Material slide 7), showing a coercive field of 20 mT and a saturation magnetization of 1.4 emu/g of the composite (this corresponds to ~70 emu/g of magnetite since the estimated weight fraction of magnetite present in the sample is ~ 2 wt%). The particles located inside the channels of size D ~ 4 nm (as determined by TEM) are superparamagnetic [10] and have negligible coercivity, but contribute to the overall magnetization of the material.

Hydrogen adsorption measurements

Hydrogen adsorption/desorption measurements were performed at 77 K on the CMK-3 and Fe-CMK-3 samples in a pressure range of 0-10 bar. The curves obtained can be seen in Figure 3.
Nonlinear least squares regression was used to fit the experimental data and a numerical optimization method (Levenberg-Marquardt) was employed. The regression coefficient of fit was 0.98, indicating good accuracy. Over the entire pressure range, the amount of adsorbed hydrogen is higher in the iron-containing sample. The process is completely reversible, as. The presence of magnetite nanoparticles increases the hydrogen adsorption capacity of CMK-3 alone. The magnetite aggregates are better dispersed aided by the surface area of CMK-3; therefore, the nanoparticles are smaller and the activity for hydrogen storage increases due to the higher surface area of magnetite nanoparticles and their high dispersion.

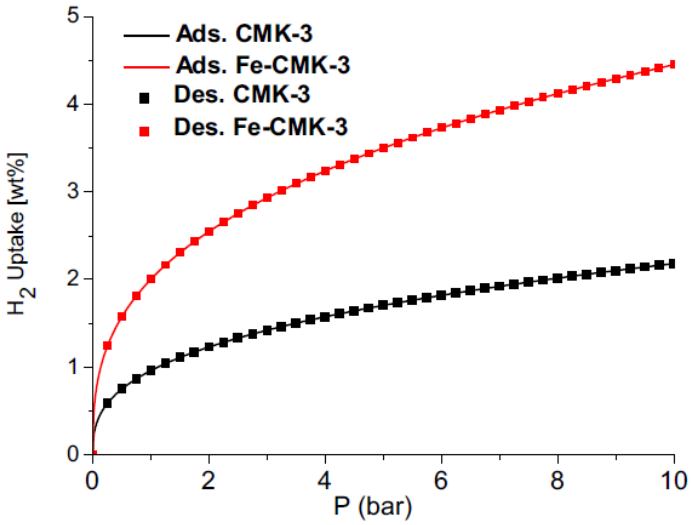

Figure 3: Hydrogen adsorption /desorption curves on CMK-3 and Fe-CMK-3 at 77 K

There are two important charge transfer mechanisms in hydrogen adsorption. On the one hand, the hydrogen molecule is a weak Lewis acid that donates charges from its σ orbital. On the other hand, it functions as a weak Lewis base where the σ* orbital of the hydrogen molecule accepts the charge of the adsorbent. An important contribution to H2 physisorption is found in the phenomenon of polarization, which creates electrostatic moments in the H2 molecule. This allows an attractive electrostatic interaction with the linker.

In this study, CMK-3 carbon acts as a support framework of magnetite nanoparticles for Kubas hydrogen bonding. According to studies [11], on Ti-decorated nanotubes, the first hydrogen molecule dissociates into two hydrides by oxidative addition to magnetite. During this process, the H-H distance increases. The second, third and fourth hydrogen molecules bind to the magnetite nanoparticle without dissociating in a Kubas-type interaction. Yildirim's [11] calculations show that the system is stable until four hydrogen molecules are adsorbed.

Therefore, this adsorption mechanism is similar to that described in this work for magnetite-decorated CMK-3 in that it uses carbon support as a grafting site for Kubas-type hydrogen bonding. Assuming weak orbital interactions between H2, and the magnetite active site, it can be assumed that the first layer of hydrogen molecules can react with dissociation on the magnetite nanoparticle. The second, third and fourth layers interact with the Fe-CMK-3 magnetite through a metal-dihydrogen Kubas complex [12]. More layers could bond with the metal oxide particles through induced dipole forces because the strong interaction between magnetite nanoparticles and hydrogen molecules induces dipole forces and more H2 molecules may be adsorbed on more layers through dipole-dipole interactions, but the binding forces decrease when the distance to the Fe-CMK-3 surface increases.

In previous work, we have studied the effect on hydrogen adsorption of different mesoporous carbons modified with different nanoparticles (Table 2) [4, 6, 13, and 14]. The hydrogen adsorption capacity depends not only on the surface area of the nanomaterial but also on the size and characteristics of the modifying nanoparticles.

Table 2 Hydrogen adsorption of different nanomaterials

Material	Hydrogen uptake (wt%)*	Reference
Pt-CMK-3	3.3	(Juárez et al. 4)
Anatase-CMK-3	2.9	(Gómez Costa et al.13)
Ti-CMK-3	2.6	(Juárez et al. 6)
VxOy-CMK-3	3.43	(Juárez et al. 14)

*H_2 sorption at 10 bars and 77 K

Conclusion

A significant result of this research related to hydrogen adsorption and storage refers to the design of ordered mesoporous carbon modified with magnetite nanoparticles. This material adsorbs hydrogen molecules through weak bond forces (physisorption). The activity of the samples are due to a high surface area of both the mesoporous carbon and the exposed surface of the magnetite nanoparticles as well as the uniform dispersion of this.

In this work, a mechanism is proposed explaining how hydrogen molecules are adsorbed on the sample and the difference in adsorption between the Fe-CMK-3 material and the support.

We are in the process of optimization and improvement of the material to increase the adsorption of hydrogen and therefore increase the storage capacity. This optimization in adsorption capacity can be done through the control of the size and dispersion of the nanoparticles and the type of support

ACKNOWLEDGEMENTS

J.M. Juarez, M. Gomez Costa, O. A. Anunziata NANOTEC, CONICET Researchers. We acknowledge the financial support of CONICET Argentina, PIP CONICET 11220120100218CO 2014–2018 and PICT-Foncyt RES 475/2015; 2017–2021.

REFERENCES

1] Giasafaki D, Bourlinos A, Charalambopoulou G, Stubos A, Steriotis TH Synthesis and characterisation of nanoporous carbon–metal composites for hydrogen storage. Microporous Mesoporous Mater (2012) 154:74–81. https://doi.org/10.1016/j.micromeso.2011.11.011

2] Giraudet S, Zhu Z Hydrogen adsorption in nitrogen enriched ordered mesoporous carbons doped with nickel nanoparticles. Carbon (2011) 49:398–405. https://doi.org/10.1016/j.carbon.2010.09.035

3] Kim BJ, Park SJ Optimization of the pore structure of nickel/graphite hybrid materials for hydrogen storage. Int J Hydrogen Ener (2011) 36:648–653. https://doi.org/10.1016/j.ijhydene.2010.09.097

4] Juárez JM, Gómez Costa MB, Anunziata OA Synthesis and characterization of Pt-CMK-3 hybrid nanocomposite for hydrogen storage. Int J Energy Res (2015) 39:128–139. https://doi.org/10.1002/er.3229

5] Juárez JM, Gómez MB, Anunziata OA, Preparation and characterization of activated CMK-1 with Zn and Ni species applied in hydrogen storage. Int J Energy Res (2015) 39:941-943

https://doi.org/10.1002/er.3298

6] Juárez JM, Ledesma BC, Gómez Costa MB, Beltramone AR, Anunziata OA Novel preparation of CMK-3 nanostructuredmaterialmodified with titania applied in hydrogen uptake and storage. Microporous and Mesoporous Mater (2017) 254:146–152. https://doi.org/10.1016/j.micromeso.2017.03.056

7] Gómez Costa MB, Juárez JM, Pecchi G, Anunziata OA Anatase–CMK-3 nanocomposite development for hydrogen uptake and storage. Bull Mater Sci (2017) 40:271–280. https://doi.org/10.1007/s12034-017-1382-4

8] Suryavanshi U, Iijima T, Hayashia A, Hayashi Y, Tanemura M Fabrication of ZnO nanoparticles confined in the channels of mesoporous carbon. Chem Eng J (2012) 179:388–393. https://doi.org/10.1016/j.cej.2011.10.087

9] Darmstadt H, Roy C, Kaliaguine S, Kim TW, Ryoo R. Surface and pore structures of CMK-5 ordered mesoporous carbons by adsorption and surface spectroscopy. Chem Mater (2003) 15:3300–3307. https://doi.org/10.1021/cm020673b

10] Upadhyay S, Parekh K, Pandey B Influence of crystallite size on the magnetic properties of Fe3O4 nanoparticles. J Alloys Compd (2016) 678:478–485. https://doi.org/10.1016/j.jallcom.2016.03.279

11] Yildirim T, Ciraci S Titanium-decorated carbon nanotubes as a potential high-capacity hydrogen storage medium. Phys Rev Lett (2005) 94:175501–117550. https://doi.org/10.1103/PhysRevLett.94.175501

12] Takasu Y, Unwin R, Tesche B, Bradshaw AM, Grunze M Photoemission from palladium particle arrays on an amorphous silica substrate. Surf Sci (1978) 77:219–232. https://doi.org/10.1016/0039-6028 (78) 90003-1

13] Juárez JM, Gómez Costa MB, Martínez ML, Anunziata OA Influence of vanadium nanoclusters in hydrogen uptake using hybrid nanostructured materials. J Porous Mater (2019) 26:951–959. https://doi.org/10.1007/s10934-018-0689-x

14] Gómez Costa MB, Juárez JM, Martínez ML, Beltramone AR, Cussa J, Anunziata OA. Synthesis and characterization of conducting polypyrrole/SBA-3 and polypyrrole/Na–AlSBA-3 composites. Mat Res Bull (2016) 48:661–667. https://doi.org/10.1016/j.materresbull.2012.11.030